IOP Publishing Journal of Physics: Conference Series **59** (2007) 5–10
doi:10.1088/1742-6596/59/1/002 Eighth International Conference on Laser Ablation

# Laser-matter interaction in the bulk of transparent dielectrics: Confined micro-explosion

**Eugene Gamaly, Barry Luther-Davies, Andrei Rode***

Laser Physics Centre,
Research School of Physical Sciences and Engineering,
the Australian National University, Canberra ACT 0200, Australia

**Saulius Joudkazis, and Hiroki Misawa**

CREST-JST and Research Institute for Electronic Science, Hokkaido University, N-21-W10, CRIS Bldg., Kita-Ku, Sapporo 001-0021, Japan

**Ludovic Hallo, Philippe Nicolai, Vladimir Tikhonchuk**

Centre Lasers Intenses et Applications, UMR 5107 CEA – CNRS - Université Bordeaux 1, 33405 Talence, Cedex, France

*avr111@rsphysse.anu.edu.au

**Abstract**. We present here the experimental and theoretical studies of drastic transformations induced by a single powerful femtosecond laser pulse tightly focused inside a transparent dielectric, that lead to void formation in the bulk. We show that the laser pulse energy absorbed within a volume of less than 1μm$^3$ creates the conditions with pressure and temperature range comparable to that formed by an exploding nuclear bomb. At the laser intensity above $6\times10^{12}$ W/cm$^2$ the material within this volume is rapidly atomized, ionized, and converted into a tiny super-hot cloud of expanding plasma. The expanding plasma generates strong shock and rarefaction waves which result in the formation of a void. Our modelling indicates that unique states of matter can be created using a standard table-top laser in well-controlled laboratory conditions. This state of matter has temperatures $\approx10^5$K, heating rate up to the $10^{18}$ K/s, and pressure more than 100 times the strength of any solid. The laser-affected sites in the bulk were detected ("read") by generation of white continuum using probe femtosecond pulses at much lower laser intensity of $10^{10}$ W/cm$^2$ – $10^{11}$ W/cm$^2$. Post-examination of voids with an electron microscope revealed a typical size of the void ranges from 200 to 500 nm. These studies will find application for the design of 3D optical memory devices and for formation of photonic band-gap crystals.

## 1. Introduction

It has been discovered recently that tightly focused femtosecond laser pulses can be used to produce three-dimensional structures with less than half-micron sizes inside a transparent medium (silica glasses, crystalline quartz and polymers) [1-7]. To achieve this, the laser beam must be focused into a volume $\sim\lambda^3$ ($\lambda$ is the laser wavelength) using high numerical aperture optics. It has been also demonstrated that these structures can be formed in different spatial arrangements [3-7]. It has been sug-

 

gested that this technique could be used for the formation of photonic crystals, waveguides and gratings for application in photonics. A single structure can also serve as a memory bit because it can be detected (or "read") through a white continuum excited by a probe laser beam [1]. We present here the results of the studies revealing the physical processes behind this phenomenon.

## 2. Experiments

A beam from a Ti:sapphire laser ($\lambda$=800 nm, 130 fs pulse duration, average intensity in excess 6.6 TW/cm$^2$) was focused into a silica glass sample using an infinity-corrected oil-immersion objective lens with numerical aperture $NA$ = 1.35 and magnification ×100 mounted in a microscope (Olympus IX70) [1]. The peak laser power (0.5 MW) was much lower than the threshold for self-focusing (several MW) and, therefore, the laser energy could be delivered to the focal volume located from 5 μm up to 50 μm below the crystal surface, without inducing damage in the region between the surface and the focus.

***Focal volume and focal spot area.*** We define the focal volume as the space inside the cylindrical volume at the surface at which the intensity equals 1/2 the maximum value. We take the axial length of focal volume to be equal to the doubled Rayleigh length $z_0 = \pi r_0^2 n / \lambda_0$. Here $\lambda_0$ is wavelength in vacuum, $n$ is the refractive index of the medium, $r_0$ is the minimum waist radius of the Gaussian beam. Expressing this radius through the numerical aperture of the lens and vacuum wavelength in accordance to [8] one obtains the focal volume as follows:

$$V_{1/2} = 0.947 \cdot \lambda_0^3 n / (NA)^4$$

Correspondingly the focal spot area is expressed as follows:

$$S_{1/2} = \pi r_{1/2}^2 = 0.405\, \lambda_0^2 / (NA)^2$$

Taking $n$ =1.5, $\lambda_0$ = 800 nm, one gets $V_{1/2}$ = 0.219 μm$^3$; $S_{1/2}$= 0.153 μm$^2$; $r_{1/2}$= 212 nm. The second and third harmonics of the same laser at an intensity 10-100 GW/cm$^2$ were used for detection of the structures so-produced via the emission of localised white light continuum (Fig. 1). This emission was recorded on a spectrometer with spectral resolution of 2 nm and temporal resolution of 13 ps. The lateral and axial sizes of the void produced in silica glass at an intensity three times higher than the damage threshold were 259 nm and 300 nm respectively. A detailed description of the experimental set-up and the measurements can be found in [1].

***Experiments with glass.*** Silica glass (viosil) was studied for the nano-void formation (Fig. 1). Viosil is transparent till 150 nm, and has the Young modulus of Y = 75 GPa. SEM examination of the irradiated region after slicing the affected area with an ion beam confirmed the formation of nanovoid for pulse energies larger than approximately 30 nJ. This energy depends on the recording depth due to spherical aberrations. A wet etching procedure was used to reveal the extent of the photo-modified region. There were no clear boundary between laser affected and unaffected regions in silica. The contrast of wet etching rates in the case of damaged vs undamaged silica was ~40. The etching rate was measured as the ratio of the channel formation along the recorded overlapping irradiated microvolumes to the widening of the channel (more details can be found elsewhere [18]). At optimized separation of the irradiated regions the width of the etched out channel corresponds to the cross-section of the photo-modified region. Typical threshold of optically recognizable modification was 13 nJ and the onset of void formation was at 30 nJ at the focus.

## 3. Optical breakdown: ionization and recombination

It is well established [9-14] that avalanche ionization, and multiphoton ionization [14] are responsible for optical breakdown in dielectrics. The process of energy absorption by electrons oscillating in he high frequency laser field can be presented as by considering Joule heating [10]:

$$\frac{d\varepsilon}{dt} = \varepsilon_{osc} \cdot \frac{\omega^2 \cdot \nu_{e-ph}}{\left(\nu_{e-ph}^2 + \omega^2\right)}$$

The electron-phonon momentum exchange rate, $\nu_{e\text{-}ph}$, can be estimated through the ionization potential [14], $J_i$,, as follows, $\nu_{e-ph} \approx \left(m^*/M\right)^{1/2} J_i/\hbar \sim 10^{14}\text{s}^{-1}$. The avalanche ionization rate in conditions of the experiments ($\omega >> \nu_{e\text{-}ph}$) then reads: $w_{avalanche} \approx \varepsilon_{osc}\nu_{e-ph}/J_i \sim 2\times10^{14}$ s$^{-1}$. The six photon ionization rate (per atom per second) taken in the form [10,14] $w_{mpi} \approx \omega n_{ph}^{3/2}\left[\varepsilon_{osc}/(2\cdot\Delta_{gap})\right]^{n_{ph}} \sim 3.5\times10^{16}$ s$^{-1}$ exceeds the avalanche rate. Here $n_{ph} = \Delta_{gap}/\hbar\omega \sim 6$ is the number of photons which an electron should absorb in order to be transferred from the valence to the conduction band. The material is rapidly ionized to a high degree (average ion charge of 4-5) in the very beginning of the laser pulse. The pulse duration appears to be the shortest of all relaxation times. Therefore all processes during the pulse time proceed in non-equilibrium conditions.

In the solid density plasma the recombination proceeds mainly by three-body collisions with one electron acting as the third body [15]. The characteristic recombination time in the conditions of the experiments is $t_{rec} = 28$ fs. The electron number density during the pulse is obtained from the rate equation where the electron sources are avalanche ionization and multi-photon ionization and recombination is due three-body collisions. The electron number density is in the range of $10^{23}$ cm$^{-3}$ < $n_e$ < $10^{24}$ cm$^{-3}$ and is in agreement with the previous calculations.

## 4. Laser modified optical properties of the ionised solid

Assuming single ionization early in the laser pulse $n_e \sim n_a \sim 10^{23}$cm$^{-3}$, one obtains plasma frequency $\omega_p^2 = 4\pi e^2 n_e/m^* = 3.74\text{x}10^{32}$ s$^{-2}$. The imaginary part of the plasma dielectric function equals to $\varepsilon'' \approx \omega_{pe}\left(1+\omega^2/\omega_{pe}^2\right)^{-1}/\omega = 8$, here $\omega = 2\pi c/\lambda_0$. The real and imaginary parts of the refractive index are of the same order, $n \approx k = \left(\varepsilon''/2\right)^{1/2} = 2$. The absorption length and the absorption coefficient are respectively: $l_{abs} \approx c/\omega k = 6.3\times10^{-6}$ cm, $A = 1-R \approx 4n\left[(n+1)^2+n^2\right]^{-1} = 0.61$. Thus, the laser energy is effectively absorbed in a volume $V_{abs} = \pi r_{1/2}^2 l_{abs}$, which is much smaller than the focal volume.

## 5. Maximum pressure in the absorption volume

In sub-picosecond laser-solid interactions, the deposited energy is confined to the electrons whilst the ions remain cold. The electron energy density in the absorption volume during the laser pulse can be estimated with all losses being neglected apart from the energy expensed in ionisation. However, because the recombination time is shorter than the pulse duration the ionisation equilibrium becomes established towards the end of the pulse. Thus, the maximum pressure by the end of the pulse can be estimated from the whole deposited energy in the absorbing volume. Taking the pulse energy $E_{Las} = 10^{-7}$ J, $S_{1/2} = 0.144$ μm$^2$, $l_{abs}$=6.3×10$^{-6}$cm; $A = 0.61$ one obtains the energy density (pressure) of $2AF_p/l_{abs} = \left(2AE_{Las}\right)/\pi r_{1/2}^2 l_{abs} = 1.26\times10^7$ J/cm$^3$. Hydrodynamic motion begins shortly after the end of the pulse. The initial pressure driving the shock wave is 12.9 TPa, and this significantly exceeds the Young's modulus: $P >> Y \sim 0.4$ TPa.

Consequently, after the end of the pulse a strong shock wave starts to propagate from the absorbing region compressing the surrounding matter while a rarefaction wave moves in the opposite direction towards the centre of symmetry. The degree of ionization reaches a state of equilibrium and the electron and ion temperature have equilibrated by the end of the pulse. Therefore, all the transient processes involving shock wave propagation, material compression and pressure release can be described in the framework of equilibrium plasma hydrodynamics.

## 6. Void formation process

The formation of a void can be understood from simple reasoning based on the laws of mass and energy conservation. Let us consider for simplicity spherically symmetric motion. The shock wave

propagating in a cold material loses it's energy due to dissipation, e.g. due to the work done against the internal pressure (Young modulus) that resists material compression. The distance at which the shock front effectively stops defines the shock-affected volume. Actually at this point the shock wave converts into a sound wave, which propagates further into the material without inducing any permanent changes to the sapphire. This distance where the shock wave stops can be estimated from the condition that the internal energy in the volume inside the shock front is comparable to the absorbed energy: $4\pi P_0 r_{stop}^3/3 \approx E_{abs}$. In other words at this position the pressure behind the shock front equals the internal pressure of the cold material. One can reasonably suggest that the sharp boundary observed between the amorphous (laser-affected) and crystalline (pristine) material corresponds to the distance where the shock wave has effectively stopped. The experimentally measured dependence of the laser-affected zone diameter, $D_a$, (outer size of amorphous region) on the laser energy can be fitted using the above argument by $D_a = l_{a0}\left(AE_{p,nJ}\right)^{0.33}$, from which we deduce $l_{a,0}$= 80 nm. This value of the characteristic length, $l_a$, at the threshold energy is in fact close the absorption depth for plasma as calculated above.

Similarly one can apply the mass conservation law to estimate the density of compressed material from the void size. Indeed, the mass conservation relates the size of the void to compression of the surrounding shell. One can use the void size from the experiments and deduce the compression of the surrounding material. The void formation inside a solid is only possible if the mass initially contained in the volume of the void was pushed out and compressed. Thus after the micro-explosion the whole mass initially confined in a volume with radius $r_a$ resides in a layer in between $r_a$ and $r_v$ which has a density $\rho = \delta\rho_0;\ \delta > 1$. The void radius can be expressed through the compression ratio and the radius of laser-affected zone with the help of mass conservation as follows:

$$r_v = r_a\left(1-\delta^{-1}\right)^{1/3}$$

Typically we observed $r_{void} \sim 0.5\times r_{stop}$ which means that amorphous material should have a density 1.14 times higher than that of the bulk.

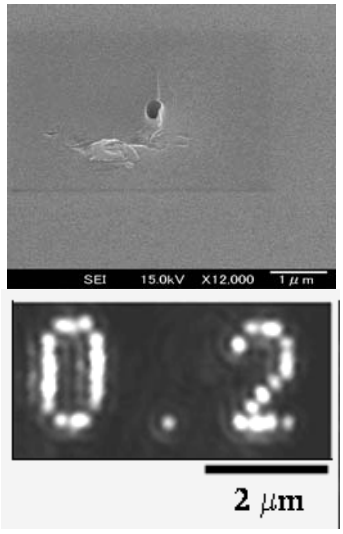


Figure 1: SEM image of axial cross sections of a 220-nm void in silica (top, scale bar 1 μm); and an example of white light continuum readout of recorded structure made of 0.2 μm voids in glass.

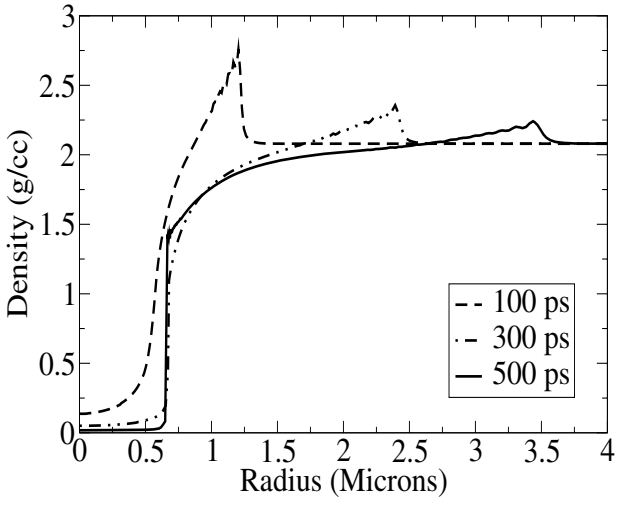


Figure 2. Density profile from two-temperature hydrodynamic simulations using code Chivas for time moments 0.1 ns, 0.3ns, and 0.5 ns after a 100 nJ laser pulse. Fast decay of the shock amplitude is clearly seen, as well as the void of $r_{void}$ ~0.7 μm formed.

## 7. Computer modeling of void formation.

The plasma created by rapid laser energy deposition in a focal volume attains local thermodynamic equilibrium in time less than 1 ps. Therefore the process of plasma expansion into a bulk can be described in frames of two-fluid hydrodynamics (ionization equilibrium, electrons and ions with separate temperatures) accompanied by electron heat conduction. The calculations were performed in spherical geometry with the hydrodynamic code Chivas [16]. We approximate the cylindrical region where the energy absorbs by the equivalent sphere, $V_{abs} = \pi r_{1/2}^2 l_{abs} = (4/3)\pi r_{dep}^3$. An energy of $10^{-7}$ J was deposited homogeneously over the spherical volume of a radius $<r>$ = 0.13 μm. The equation of state (EOS) implemented in the code [17] describes solid-melt-plasma transitions in correspondence with experiments. Using this EOS one can estimate the temperature reached at the end of the laser pulse and the average ion charge, taking into account the energy losses for phase transitions and ionisation; the estimates give $T_e$ = 26.2 eV and average ionization (the number of stripped electrons) $<Z>$ = 4.3.

Hydrodynamic motion begins when electrons transfer the excess of the absorbed laser energy, left after the breaking the inter-atomic bonds, to the ions. The strong shock wave emerges at the outer surface of energy deposition sphere compressing the material to a density twice of the initial one. The pressure behind the shock front rapidly decreases with the distance and finally transforms into an acoustic wave. A void is then formed behind the shock wave and the void radius gradually increases to its final value (see figure 2). The spatial density profiles for the time moments 0.1, 0.3, 0.5 ns are shown in figure 2. The compression ratio at 1 ns time reaches its asymptotic value of $\delta = (\rho/\rho_0) = 1.1$ which qualitatively complies with the density of amorphous layer retrieved from experiments, $\delta_{exp} = 1.14$. The different models used in computer simulations give the same qualitative features of shock emergence, propagation, and void formation allowing for identification of the effects (heat conduction is most important) that are essential for quantitative description of experiments. We note that the remaining gas density in the void at 1 ns time is above 0.1 g/cm$^3$.

## 8. Conclusion

To conclude, we generated and analyzed extreme conditions created by a single pulse table-top femtosecond laser inside a bulk transparent dielectric which results in the formation of voids. The laser-affected zone formed by 100 nJ pulse is about 500nm, about twice the size of the void formed in the center. Studies of the tightly focused laser inside the transparent solid encompass an exciting field for both applied and fundamental science. Obvious applications of micro-void formation are in controlled formation of 3D structures for photonics and optical memory.

## References


[1] S. Juodkazis, A. V. Rode, E. G. Gamaly, S. Matsuo, H. Misawa, Recording and reading of three-dimensional optical memory in glasses*, Appl. Phys. B* **77**, 361-368 (2003).

[2] C. B. Schaffer, J. F. Garcia, E. Mazur, Bulk heating of transparent materials using a high-repetition rate femtosecond laser, *Appl. Phys. A* **76**, 351-354 (2003).

[3] H. Misawa, *Electronics Weekly* (UK) **5**, 10, (1995).

[4] E. N. Glezer, M. Milosavjevic, L. Huang, R. J. Finlay, T.-H. Her, J. P. Callan, E. Masur, *Opt. Lett.* **21**, 2023-2026 (1996).

[5] M. Watanabe, H. Sun, S. Juodkazis, T. Takahashi, S. Matsuoto, Y. Suzuki, J. Nishi, H. Misawa, *Jpn. J. Appl. Phys.* **37**, L1527 (1998).

[6] J. Qiu, K. Miura, H. Inouye, J. Nishi, K. Hirao *Nucl. Instrum. Methods Phys. Res. B*, **141**, 699 (1998).

[7] S. Juodkazis, T. Kondo, V. Mizeikis, S. Matsuo, H. Misawa, E. Vanagas, I. Kudryashov, in; *Proc. Bi-lateral Conf. Optoelectronic and Magnetic Materials*, Taipei, ROC, 25-26 May 2002, pp. 27-29 (2002); (available as arXiv: physics/0205025v19 May 2002).

[8] M. Born and E. Wolf, *Principles of Optics*, Cambridge, 7th ed., 2003

[9] E. Yablonovitch and N. Bloembergen *Phys. Rev. Lett.*, **29**, 907-910 (1972).

[10] Yu.P. Raizer, *Laser-induced Discharge Phenomena* (Consultant Bureau, New York, 1977).

[11] D. Arnold and E. Cartier, *Phys. Rev. B*, 46(23), 15102-15115 (1992).
[12] B.C. Stuart, M.D. Feit, A.M. Rubenchick, B. W. Shore, and M. D. Perry *Phys. Rev. Lett*, **74**, 2248-2251 (1995).
[13] D. von der Linde and H. Schuler, Breakdown threshold and plasma formation in femtosecond laser-solid interaction *JOSA B*,13(1), 216-222 (1996).
[14] Yu.A. Il'inski and L.V. Keldysh, *Electromagnetic response of Material Media*, (Plenum Press, 1994).
[15] Ya.B. Zel'dovich and Yu. P. Raizer, *Physics of Shock Waves and High-Temperature Hydrodynamic Phenomena*, (Dover, New York, 2002).
[16] S. Jacquemot and A. Decoster, *Laser and Particle Beams* **9**, 517 (1991).
[17] R. M. More, K. H. Warren, D. A. Young and G. B. Zimmerman, *Phys. Fluids* **31**, 3059 (1988).
[18] S. Juodkazis, K. Yamasaki , V. Mizeikis, S. Matsuo and H. Misawa *Appl. Phys. A*, 1549 – 1553 (2004).